NEOPLASIA
www.neoplasia.com

Volume 21 Number 8 August 2019 pp. 788–801 788

Overcoming Tyrosine Kinase Inhibitor Resistance in Transformed Cell Harboring *SEPT9-ABL1* Chimeric Fusion Protein

Hidetsugu Kawai[*,†], Hiromichi Matsushita[*,‡], Rikio Suzuki[*,†], Yuka Kitamura[*], Yoshiaki Ogawa[†], Hiroshi Kawada[*,†] and Kiyoshi Ando[*†]

[*]Research Center for Cancer Stem Cell, Tokai University School of Medicine, Isehara, Kanagawa, Japan; [†]Department of Hematology/Oncology, Tokai University School of Medicine, Isehara, Kanagawa, Japan; [‡]Division of Pathology and Clinical Laboratories, National Cancer Center Hospital, Tokyo, Japan

Abstract

Hematological malignancies harboring various ABL1 fusions are expected to be sensitive to tyrosine kinase inhibitors (TKIs), similar to those with BCR-ABL1. However, SEPT9-ABL1 exhibits TKI resistance both *in vitro* and *in vivo*. SEPT9-ABL1 has the same ABL1 region as seen in BCR-ABL1 but no point mutation in its kinase domain, which is one of the main mechanisms underlying TKI resistance in the leukemic cells harboring BCR-ABL1. The purpose of this study was to reveal the mechanism underlying TKI resistance induced by SEPT9-ABL1. We focused on the TP53 status because TKI-induced apoptosis in BCR-ABL1–positive cells is achieved through TP53. Mouse TP53 homologue TRP53 was downregulated and less phosphorylated in the cells expressing SEPT9-ABL1 than in those with BCR-ABL1, resulting in the prevention of apoptosis induced by TKIs. The CRM1 inhibitor KPT-330 accumulated nuclear TRP53 and NFKB1A (also known as IκBα), which is thought to capture TRP53 in the cytoplasm, and induced apoptosis in the hematopoietic cells expressing SEPT9-ABL1. In addition, the combination treatment of KPT-330 and imatinib, which induced the marked nuclear accumulation of PP2A and SET, reactivated PP2A through its dephosphorylation and inhibited SET expression, resulting in the effective induction of the apoptosis in the cells expressing SEPT9-ABL1. The combination treatment with KPT-330 and imatinib successfully reduced the subcutaneous masses expressing SEPT9-ABL1 and extended the survival of the mice intraperitoneally transplanted with SEPT9-ABL1–expressing cells. These results show that therapy with CRM1 inhibitors may be effective for overcoming TKI resistance induced by SEPT9-ABL1.

Neoplasia (2019) 21, 788–801

Introduction

The fusion gene *BCR-ABL1* is derived from t(9;22)(q34;q11.2), which is detected in patients with chronic myeloid leukemia (CML) and approximately 30% of patients with acute lymphoblastic leukemia (ALL) [1]. BCR-ABL1 is believed to contribute to leukemogenesis through tyrosine kinase activity from the ABL1 region that activates multiple downstream signals [2]. Tyrosine kinase inhibitors (TKIs), such as imatinib, dasatinib, and nilotinib, have been developed to target BCR-ABL1 and reportedly induce hematological remission in patients with CML immediately, resulting in the dramatic improvement of their prognosis [3,4]. TKIs are also effective for treating *BCR-ABL1*–positive ALL, and the prognosis of such patients has been improved in combination with chemotherapy and stem cell transplantation [5]. Therefore, TKIs against BCR-ABL1 are a representative paradigm of molecular-targeted therapy for malignancies.

Infrequently, *ABL1* fusions that are fused to genes other than *BCR* are found in various hematological malignancies [6]. Because they share the ABL1 molecule in common, they are expected to be

Address all correspondence to: Hiromichi Matsushita, Division of Pathology and Clinical Laboratories, National Cancer Center Hospital, 5-1-1 Tsukiji, Chuo-ku, Tokyo 104-0045, Japan. E-mail:; hirommat@ncc.go.jp
Received 10 March 2019; Revised 3 June 2019; Accepted 4 June 2019

1476-5586
https://doi.org/10.1016/j.neo.2019.06.001

sensitive to TKIs. NUP214-ABL1, which is typically detected in T-cell acute lymphoblastic leukemia (T-ALL), has been found to be sensitive to TKIs *in vitro*, *in vivo*, and clinically [7]. In ar ABL1 fusions have been reported to be sensitive to TKIs.

We previously identified the fusion gene *SEPT9-ABL1* in a patient with T-prolymphocytic leukemia (T-PLL) [8]. SEPT9 is a GTP-binding protein ubiquitously expressed and considered to be a component of cytoskeletal structures [9]. We have proven that SEPT9-ABL1 exhibits TKI resistance *in vitro* and *in vivo*, as seen in the clinical course [8,10]. Point mutations in the kinase domain of the BCR-ABL1 product are one of the main mechanisms underlying the development of TKI resistance [11]. However, SEPT9-ABL1 has no point mutations in the ABL1 region. As such, the mechanisms underlying the TKI resistance in the cells harboring SEPT9-ABL1 remain unclear.

It has been reported that the tumor suppressor TP53 is one of the molecules responsible for the antileukemic effect of TKIs on BCR-ABL1–positive cells [12]. TP53 is stabilized through tetramer formation by the phosphorylation of Ser 392 [13] and transcriptionally regulates genes involved in DNA repair, cellular senescence, and apoptosis. In malignant cells, TP53 is often inactivated by mutations in its exons or removed by pathophysiological mechanisms, including mouse double minute 2 (MDM2) oncoprotein that promotes the nuclear export and degradation of TP53 [14,15].

The purpose of this study was to clarify the mechanism underlying TKI resistance in cells harboring SEPT9-ABL1. We focused on analyzing the TP53 status of these cells in comparison to that of cells harboring BCR-ABL1 which is a typical example of a TKI-sensitive ABL1 fusion.

Materials and Methods

Patient Samples

The patient's frozen bone marrow samples were obtained after written informed consent was provided in accordance with the Declaration of Helsinki and with approval from the Tokai University Committee on Clinical Investigation (permit number: #15I-26). Other samples were obtained from the untreated patients with chronic myeloid leukemia in blastic crisis (CML-BC) and B-cell ALL patients harboring the *BCR-ABL1* fusion gene, as well as a T-PLL patient harboring *SEPT9-ABL1*.

Cell Culture, Retroviral Infection

A packaging cell line consisting of Plat-gp cells (a generous gift from Prof. Toshio Kitamura, Institute of Medical Science, University of Tokyo) was cultured in DMEM containing 10% fetal bovine serum (FBS) at 37°C under 5% CO_2. The transduction of the plasmids into attached cells to produce viral supernatant was performed using Fugene HD (Promega, Madison, WI), according to the manufacturer's protocol.

32D cells and BaF3 cells, a murine interleukin-3 (IL-3)–dependent hematopoietic cell line, were cultured in RPMI 1640 medium containing 10% FBS and recombinant murine IL-3 (5 ng/ml) at 37°C under 5% CO_2. One of the SEPT9-ABL1 isoforms (SEPT9f-ABL1) and BCR-ABL1 were retrovirally transduced into 32D and BaF3 cells to generate 32D/SEPT9-ABL1, 32D/BCR-ABL1, BaF3/SEPT9-ABL1, and BaF3/BCR-ABL1 cells, as previously described [16].

Chemicals

The CRM1 antagonist, termed a selective inhibitor of nuclear export (SINE), KPT-330 (Selleck Chemicals, Houston, TX) and imatinib (Santa Cruz Biotechnology, Dallas, TX) were dissolved in DMSO at 50 mM for KPT-330 and 100 mM for imatinib. The selective casein kinase 2 (CK2) inhibitor tetrabromobenzotriazole (TBB) (Abcam, Cambridge, MA) and the MDM2 antagonist Nutlin-3a (Sigma-Aldrich, St. Louis, MO) were dissolved in DMSO at 100 mM for TBB and 30 mM for Nutlin-3a. These solutions were then aliquoted and stored at −80°C.

Cell viability Assay, Establishment of IC_{50} Values

To evaluate the drug sensitivity, 10,000 cells were cultured in 96-well plates with increasing concentrations of imatinib or KPT-330. After 48 hours, the cell proliferation was evaluated using a Cell Titer-Glo Luminescent cell viability assay (Promega).

Apoptosis Assay

32D and BaF3 cells were co-incubated with Annexin V-fluorescein isothiocynate (FITC) and propidium iodide (PI) for 24 hours using the Annexin V-FITC Apoptosis Detection Kit (BD Biosciences, San Jose, CA) according to the manufacturer's protocol. Analyses were performed using BD LSRFortessa (BD Biosciences), and Annexin V/PI double-positive cells were regarded as apoptotic cells.

Western Blot Analyses

Total cell lysates prepared using RIPA buffer were electrophoresed and transferred to polyvinylidene fluoride membranes. Intranuclear or intracytoplasmic protein was fractionated and extracted using a ProteoExtract Subcellular Proteome Extraction Kit (Merck Millipore, Darmstadt, Germany) and then blocked in 0.5% Tween 20 (TBST) containing 5% milk, incubated with diluted primary and secondary antibodies, and visualized with Immobilon Western Chemiluminescent HRP Substrate (Millipore) or ECL prime (GE Healthcare, Chicago, IL). The antibodies used were as follows: anti-ACTB from Sigma-Aldrich; anti–c-Abl, anti–phospho-TP53 (Ser392), anti-TP53, anti–phospho-MDM2 (Ser166), anti–protein phosphatase type 2A (PP2A), anti-NFKB1A, anti-CRM1, anti–Lamin A/C, and horseradish peroxidase (HRP)–conjugated anti-rabbit IgG from Cell Signaling (Boston, MA); anti-MDM2 and anti–T-cell lymphoma invasion and metastasis 1 protein (TIAM1) from Santa Cruz; anti-SET from Abcam (Cambridge, MA); anti-phospho-PP2A from R&D Systems (Minneapolis, MN); and HRP-conjugated anti-mouse IgG from GE Healthcare. The protein expression was analyzed using the CS Analyzer software program, ver.3.0 (Atto Corp., Tokyo, Japan).

In Vivo Tumor Models

In subcutaneous model, 5×10^6 BaF3/SEPT9-ABL1 cells were syngeneically transplanted into BALB/c mice. The treatment was started 10 days after cell implantation. Mice were orally treated with imatinib 20 mg/kg daily, KPT-330 5 mg/kg 3 times/week or imatinib 20 mg/kg daily, plus KPT-330 5 mg/kg 3 times/week. The diameters of the subcutaneous tumors were measured twice a week, and the tumor volume ( ) was calculated using the following formula for estimation: $V = (W^2 \times L)/2$ (V: tumor volume, W: short diameter, L: long diameter).

In the intraperitoneal model, 2×10^6 BaF3/SEPT9-ABL1 or 32D/SEPT9-ABL1 cells were transplanted into BALB/c nude mice. The treatment was started the day after the cell implantation. Mice were orally treated with imatinib 20 mg/kg daily, KPT-330 50 mg/kg 3 times/week, or imatinib 20 mg/kg daily plus KPT-330 50 mg/kg 3 times/week. Moribund mice were humanly sacrificed and

evaluated histopathologically to confirm the infiltration of transplanted cells into the bone marrow, spleen, and liver using hematoxylin-eosin staining.

All experiments using animals were approved by the animal care committee of Tokai University (permit number: #171025), and all experiments were performed in accordance with the relevant guidelines and regulations.

Statistical Analyses

The significance of the differences between two groups was determined by the Mann-Whitney test. The survival curve was evaluated by the Kaplan-Meier method. These analyses were performed using the SPSS statistics software program, ver. 24 (IBM, Tokyo, Japan). Values with $P < .05$ were considered to be statistically significant.

Results

TKI Resistance Induced by SEPT9-ABL1

SEPT9-ABL1 possesses a proline-rich region along with a small part of the CDC/Septin domain from SEPT9, which is important for hetero-oligomerization between SEPT9 and other proteins, in the N-terminus and the SH3, SH2, and SH1 domains with a C-terminal structure identical to that of BCR-ABL1 in the C-terminus (Figure 1*A*). Our previous study revealed that SEPT9f-ABL1 exerted the strongest oncogenic activities among SEPT9-ABL1 isoforms [10]. Therefore, this isoform was utilized in this study to represent SEPT9-ABL1.

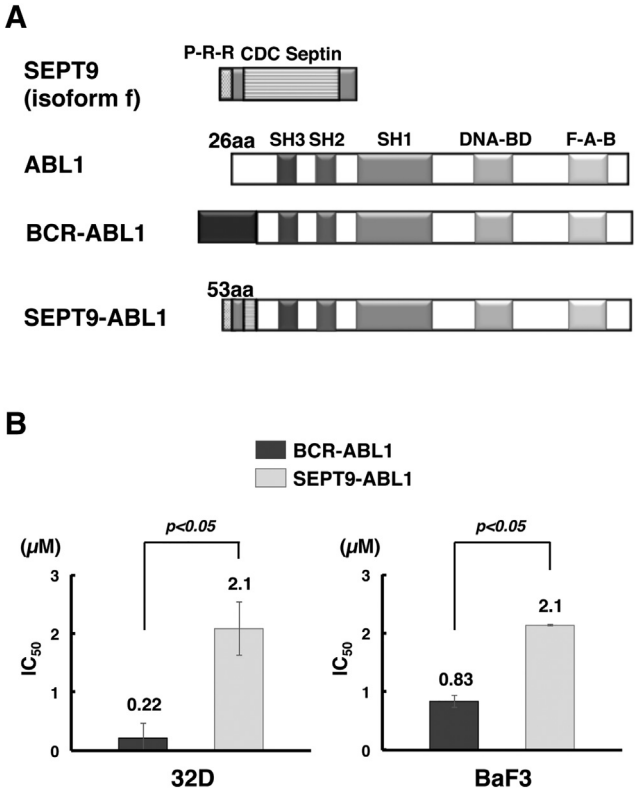

Figure 1. TKI responsiveness induced by SEPT9-ABL1.(A) The structures of BCR-ABL1 and SEPT9-ABL1. Isoform f is shown as a representative of SEPT9. The number of amino acids is also indicated. aa, amino acid; DNA-BD, DNA binding domain; F-A-B, F-actin binding; P-R-R, proline-rich region; SH, SRC homology.(B) The IC_{50} of imatinib in 32D and BaF3 cells expressing BCR-ABL1 or SEPT9-ABL1. The cells were analyzed at 48 hours after starting culture with various concentrations of imatinib.

The 50% inhibitory concentration (IC_{50}) of imatinib was higher with the expression of SEPT9-ABL1 than with that of BCR-ABL1 in 32D and BaF3 cells (Figure 1*B*). The resistance was 9.5-fold in 32D/SEPT9-ABL1 and 2.5-fold in BaF3/SEPT9-ABL1. These results confirmed that SEPT9-ABL1 contributed to TKI resistance, as seen in our previous study [10].

The Low Expression of TP53 in Hematopoietic Cells Harboring SEPT9-ABL1

To analyze the mechanisms underlying the TKI resistance in SEPT9-ABL1–expressing cells, we first analyzed the expression and phosphorylation status of TP53 in the patients' samples with ABL1 fusions using Western blotting. The TP53/ACTB and phosphorylated TP53/ACTB ratios of case 5, who was diagnosed with T-PLL harboring SEPT9-ABL1 [8], were lower than in the patients who were diagnosed with CML-BC (case 1) and ALL harboring BCR-ABL1 (cases 2 to 4) (Figure 2*A*). Consistent with these data, TRP53, a mouse homologue of TP53, was downregulated and less phosphorylated in 32D/SEPT9-ABL1 than in 32D/BCR-ABL1 (Figure 2*B*). The phosphorylation status of TRP53 in BaF3 cells also showed the same tendency using infected BaF3 cells (Figure 2*C*). Sequence analyses confirmed that 32D and BaF3 cells did not have any point mutations in the *Trp53* gene (data not shown).

The expression and phosphorylation status of MDM2, a major TP53 regulator, were then analyzed in 32D and BaF3 cells expressing BCR-ABL1 or SEPT9-ABL1. MDM2 was phosphorylated in these cells. When the cells were treated with imatinib, MDM2 was dephosphorylated in 32D/BCR-ABL1 and BaF3/BCR-ABL1. In contrast, the phosphorylation of MDM2 and the decreased expression and phosphorylation of TRP53 were sustained in 32D/SEPT9-ABL1 up to 5 μM and in BaF3/SEPT9-ABL1 up to 10μM of imatinib treatment (Figure 2, *B* and *C*).

When the cell pellets under imatinib treatment were fractionated in order to assess the cellular TRP53 distribution, the nuclear TRP53 expression was lower in 32D/SEPT9-ABL1 than in 32D/BCR-ABL1 at each concentration of imatinib (Figure 2*D*). The nuclear expression status of TRP53 in BaF3 cells also showed the same tendency using infected BaF3 cells (Figure 2*E*). These findings suggest that SEPT9-ABL1 suppressed the phosphorylation and nuclear expression of TRP53, even at elevated imatinib concentrations, probably by maintaining MDM2 phosphorylation, in order to prevent apoptosis induced by imatinib.

The Effect of a CRM1 Inhibitor on Cells Harboring SEPT9-ABL1 In Vitro

To explore ways to overcome TKI resistance in cells harboring SEPT9-ABL1, two types of agents were examined. One was the selective CK2 inhibitor TBB. It has been reported that the kinase activity of CK2 is regulated by BCR-ABL1 and that CK2 is related to TKI resistance through S6RP hyperphosphorylation and PTEN inactivation [16]. The other was the MDM2 antagonist Nutlin-3a, which inhibits MDM2-TP53 interactions and stabilizes the TP53 protein, thereby inducing cell cycle arrest and apoptosis [17]. However, the administration of these agents combined with or without imatinib did not inhibit the proliferation of 32D/SEPT9-ABL1 (data not shown).

We next focused on the nuclear export of TP53. Chromosomal region maintenance 1 (CRM1, also known as XPO1) is a ubiquitous nuclear export receptor protein of the karyopherin-β family that contributes to the nuclear export of more than 200 proteins [18,19]. CRM1 inhibitors have been reported to suppress the nuclear export of TP53 and induce its nuclear accumulation [20–22]. When a CRM1 inhibitor KPT-330 was administered, BCR-ABL1 and SEPT9-ABL1 showed similar IC_{50} without significant differences in both 32D and BaF3 cells (Figure 3*A*), with the modest effect on the alteration of the CRM1 expression (Figure 3*B*). We therefore examined the effect of KPT-330 on the hematopoietic cells expressing SEPT9-ABL1.

To determine whether or not KPT-330 inhibited transport of TRP53 by CRM1, we evaluated the intracellular distribution of TRP53 using 32D/BCR-ABL1 and 32D/SEPT9-ABL1. The basal expression of TRP53 without any treatment was higher in 32D/BCR-ABL1 than in 32D/SEPT9-ABL1. Imatinib did not inhibit but rather promoted the nuclear export of TRP53. However, KPT-330 induced the marked nuclear accumulation of TRP53 in the 32D/SEPT9-ABL1 as well as 32D/BCR-ABL1. The nuclear TRP53 accumulation was also induced by the combination treatment with KPT-330 and imatinib in both 32D/BCR-ABL1 and 32D/SEPT9-ABL1, dependent on the effect of imatinib, although the amount of nuclear TRP53 was less than noted with the treatment with KPT-330 alone (Figure 3*C*).

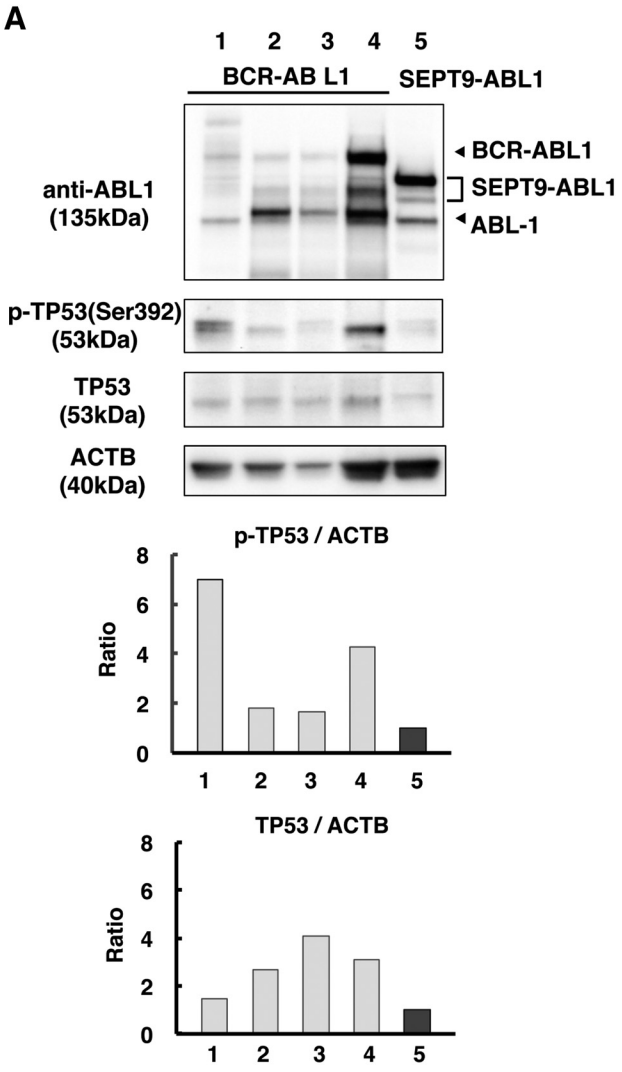

Figure 2. TP53 expression in BCR-ABL1 and SEPT9-ABL1.(A) The TP53 expression in the patient samples harboring BCR-ABL1 and SEPT9-ABL1 using a Western blot analysis. Case 1, CML-BC; cases 2 to 4, ALL harboring BCR-ABL1; case 5, T-PLL harboring SEPT9-ABL1. The phosphorylated TP53 (p-TP53)/ACTB ratio and TP53/ACTB ratio is shown below.(B, C) The mouse TP53 homologue TRP53 and MDM2 expression and phosphorylation in 32D cells (B) and BaF3 cells (C) harboring BCR-ABL1 or SEPT9-ABL1. The protein expression after treatment with imatinib (0, 1, 5, and 25 μM for 32D cells; 0, 1, and 10 μM for BaF3 cells) for 3 hours was evaluated by a Western blot analysis. Each Western blot analysis was repeated three times, and the representative images are shown. In B and C, the ratios of phosphorylated TRP53 (p-TRP53)/ACTB, TRP53/ACTB, phosphorylated MDM2 (p-MDM2)/ACTB, and MDM2/ACTB shown below were calculated using all of the analyzed data. The arrows and asterisks indicate the specific and nonspecific bands, respectively.(D, E) The cellular distribution of TRP53 in 32D cells (D) and BaF3 cells (E)expressing BCR-ABL1 and SEPT9-ABL1. The TRP53 expression after treatment with imatinib (0, 1, and 10 μM) for 8 hours was evaluated by a Western blot analysis. Each Western blot analysis was repeated three times, and the representative images are shown. The arrows and asterisks indicate the specific and nonspecific bands, respectively.

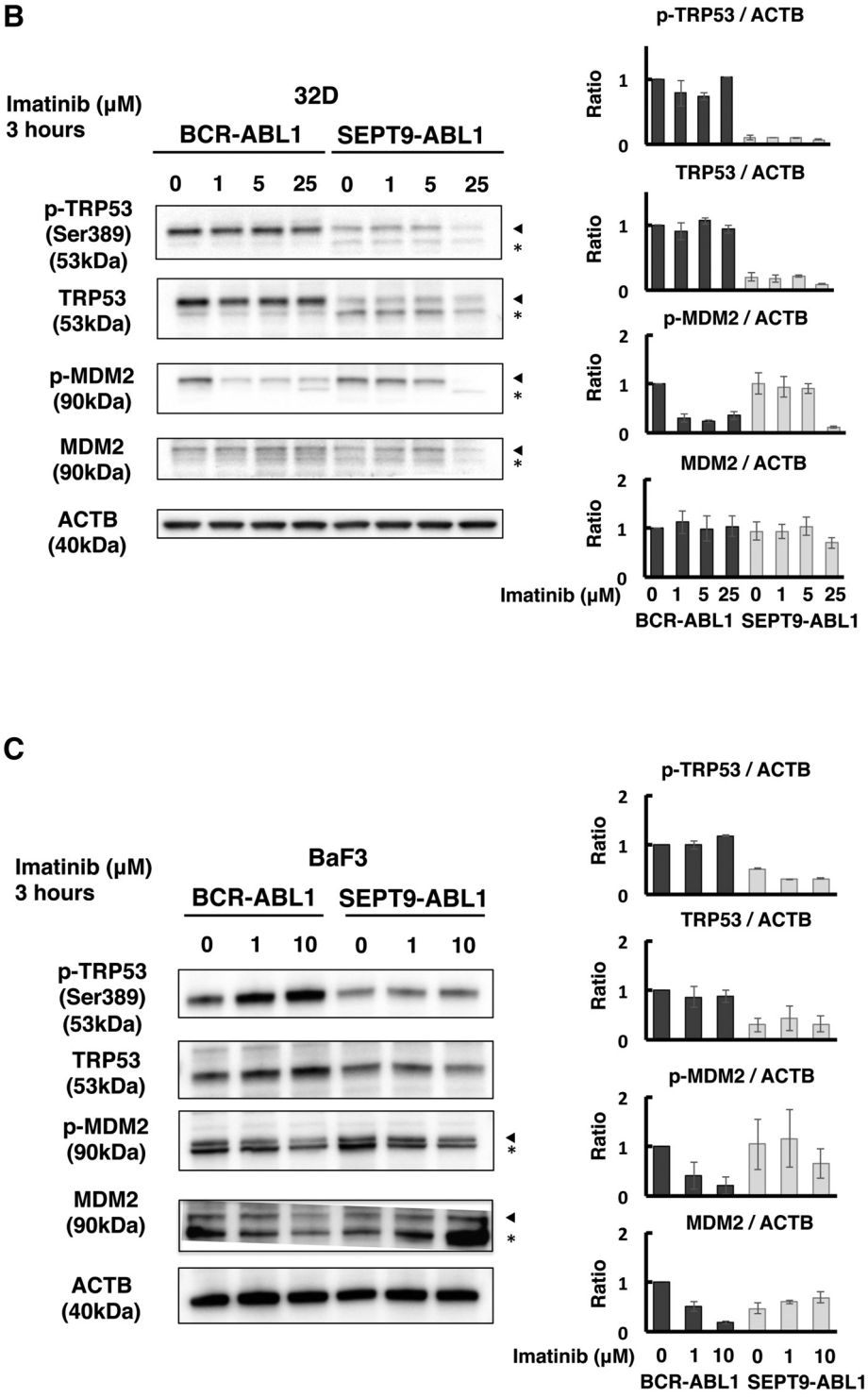

Figure 2. (*continued.*)

Regarding the nuclear accumulation of TRP53 with KPT-330 treatment, we also analyzed the intracellular distribution of NFKB1A (also known as IκBα) in these cells because BCR-ABL1 has been reported to promote the nuclear exclusion of TP53 through interaction with cytoplasmic NFKB1A, which has been reported to accumulate in the nucleus through CRM1 inhibition in CML and malignant lymphomas [23–26]. As expected, nuclear NFKB1A accumulated in 32D/BCR-ABL1 as well as 32D/SEPT9-ABL1 under treatment with KPT-330. Combination treatment with KPT-330 and imatinib further induced the nuclear accumulation of NFKB1A in 32D/SEPT9-ABL1 (Figure 3*D*).

We then focused on the tumor suppressor PP2A and BCR-ABL1–induced PP2A inhibitor SET, whichhave been also reported to accumulate in the nucleus in CML-BC cells with KPT-330 treatment, resulting in their apoptosis [27]. Imatinib treatment has been reported to induce the reactivation of PP2A, which is inhibited by the SET expression [28]. We first analyzed the phosphorylation status of PP2A and the SET expression in 32D/BCR-ABL1 and 32D/

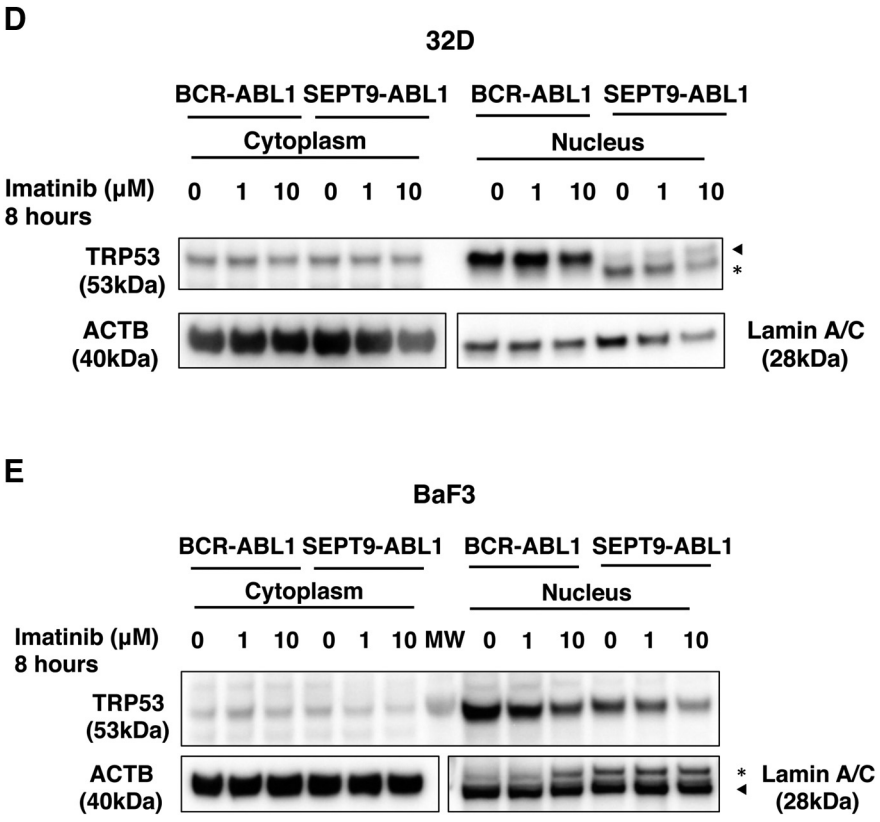

Figure 2. (*continued.*)

SEPT9-ABL1 treated with KPT-330. Imatinib induced the PP2A reactivation characterized by its dephosphorylation, and it also inhibited the SET expression in 32D/BCR-ABL1, where a considerable amount of nuclear TRP53 accumulation was detected, but did not induce these effects in 32D/SEPT9-ABL1, where less nuclear TRP53 accumulation was detected. KPT-330 alone induced neither the PP2A reactivation nor the inhibition of SET expression in both 32D/BCR-ABL1 and 32D/SEPT9-ABL1. The combination

Figure 3. The effect of the CRM1 inhibitor KPT-330 on SEPT9-ABL1 *in vitro*.(A) The IC_{50} and the dose-response curve of the CRM1 inhibitor KPT-330 in 32D and BaF3 cells expressing BCR-ABL1 or SEPT9-ABL1. The cells were analyzed at 48 hours after starting culture with various concentrations of KPT-330. These experiments were repeated five times, and the median values of IC_{50} are shown. Additionally, the representative dose-response curves are shown.(B). The CRM1 expression in 32D cells expressing BCR-ABL1 and SEPT9-ABL1. After culture without treatment for controls or with treatment of imatinib 1 μM, KPT-330 1 μM, or the combination of imatinib and KPT-330 for 24 hours, the protein expression was evaluated by a Western blot analysis. These experiments were performed three times.(C) The cellular TRP53 distribution in 32D/BCR-ABL1 and 32D/SEPT9-ABL1 treated with KPT-330. After culturewithout treatment for controls or with treatment of imatinib 1 μM, KPT-330 1 μM, or combination of imatinib and KPT-330 for 4 hours, the cells were fractionated and evaluated by a Western blot analysis. These experiments were performed three times, and the representative images are shown.(D) The cellular distribution of NFKB1A in 32D cells expressing BCR-ABL1 and SEPT9-ABL1. After culture without treatment for controls or with treatment of imatinib 1 μM, KPT-330 1 μM, or the combination of imatinib and KPT-330 for 24 hours, the cells were fractionated and evaluated by a Western blot analysis. These experiments were performed three times.(E) The PP2A phosphorylation and SET expression in 32D/BCR-ABL1 and 32D/SEPT9-ABL1 treated with KPT-330 and/or imatinib. After culture without treatment for controls or with treatment of imatinib 1 μM, KPT-330 10 μM, or combination of imatinib and KPT-330 for 24 hours, the protein expressions were evaluated by a Western blot analysis. These experiments were performed three times, and the representative images are shown. The arrows and asterisks indicate the specific and nonspecific bands, respectively. The bars below the images indicated the ratio of p-PP2A/ACTB, PP2A/ACTB, and SET/ACTB in comparison with those from untreated controls in 32D/BCR-ABL1 and 32D/SEPT9-ABL1, whichwere calculated from all the analyzed data. * indicates a *P* value <.05.(F) The cellular distribution of PP2A and SET in 32D cells expressing BCR-ABL1 and SEPT9-ABL1. After culture without treatment for controls or with treatment of imatinib 1 μM, KPT-330 1 μM, or the combination of imatinib and KPT-330 for 24 hours, the cells were fractionated and evaluated by a Western blot analysis. These experiments were performed three times. The arrows and asterisks indicate the specific and nonspecific bands, respectively.(G) The TIAM1 expression in 32D/BCR-ABL1 and 32D/SEPT9-ABL1 treated with KPT-330 and/or imatinib. After culture without treatment for controls or with treatment of imatinib 1 μM, KPT-330 1 μM, or combination of imatinib and KPT-330 for 24 hours, the protein expression was evaluated by a Western blot analysis.(H, I) The frequency of Annexin V and PI double-positive cells in 32D cells (D) and BaF3 cells (E) harboring BCR-ABL1 or SEPT9-ABL1 that were cultured without treatment or with imatinib 1 μM, KPT-330 1 μM, or the combination of imatinib 1 μM and KPT-330 1 μM. The analyses were performed 24 hours after treatment using a flow cytometry. These experiments were performed five times. * indicates a *P* value <.05.

treatment with KPT-330 and imatinib modestly induced the PP2A reactivation and inhibited the SET expression in both 32D/BCR-ABL1 and 32D/SEPT9-ABL1 (Figure 3*E*).

We therefore analyzed the intracellular distribution of PP2A and SET in 32D/BCR-ABL1 and 32D/SEPT9-ABL1 when they were treated with KPT-330. Imatinib induced the nuclear accumulation of PP2A and SET in 32D/BCR-ABL1 but not in 32D/SEPT9-ABL1. In contrast, KPT-330 induced the nuclear accumulation of PP2A and SET in 32D/BCR-ABL1 as well as 32D/SEPT9-ABL1. The combination treatment with KPT-330 and imatinib further induced the nuclear accumulation of PP2A and SET in 32D/BCR-ABL1. In 32D/SEPT9-ABL1, the amount of the nuclear PP2A was comparable in the combination treatment and KPT-330 alone (Figure 3*F*). The expression of TIAM1, the activation of which is reported to be associated with the proliferation of CLL and to cause resistance to fludarabine [29] and which is reportedly destabilized by PP2A [30], was also decreased in 32D/BCR-ABL1 and 32D/SEPT9-ABL1, in accordance with the nuclear accumulation of PP2A induced by treatment with KPT-330 alone as well as by combination treatment with KPT-330 and imatinib (Figure 3*G*). Furthermore, the amount

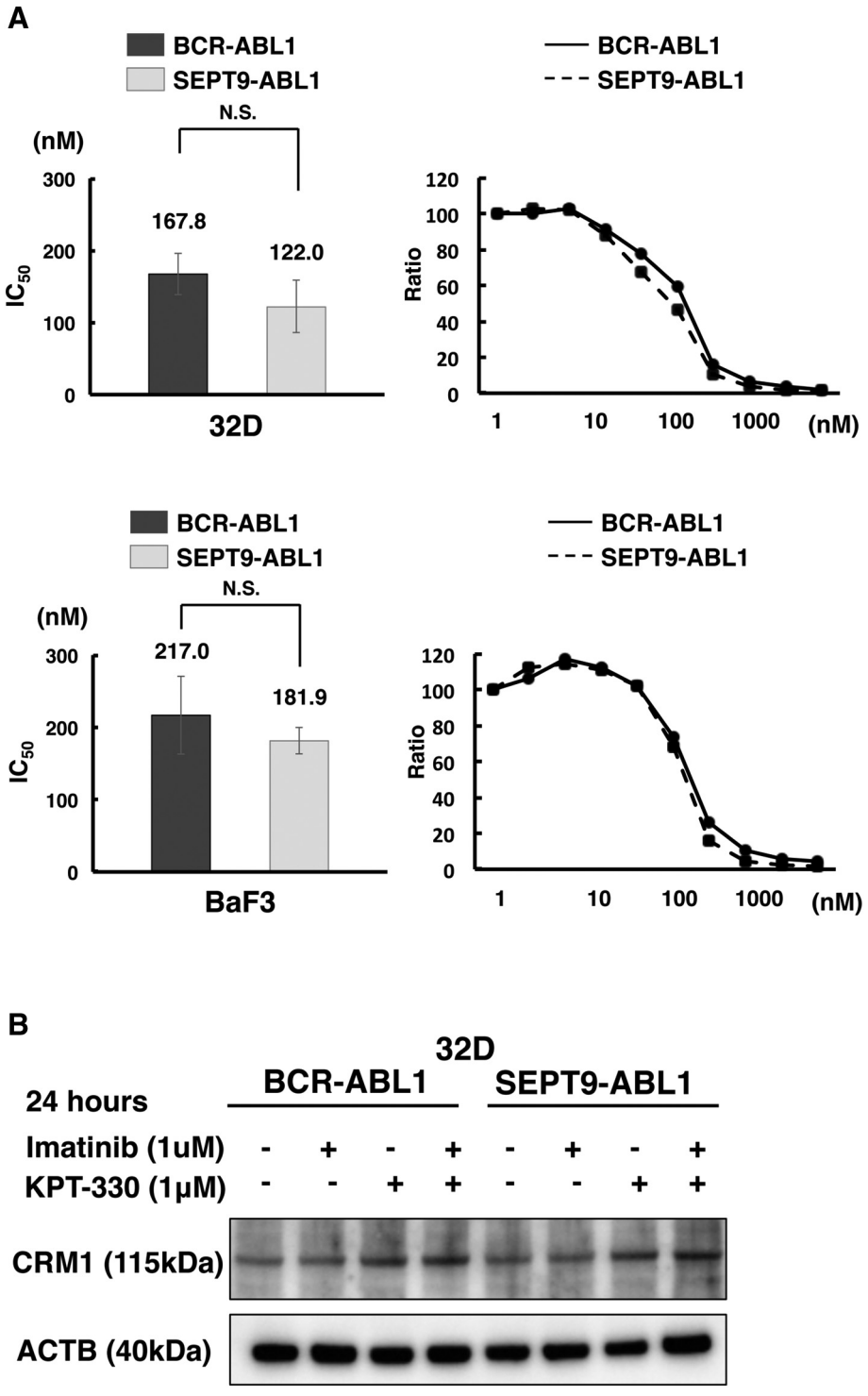

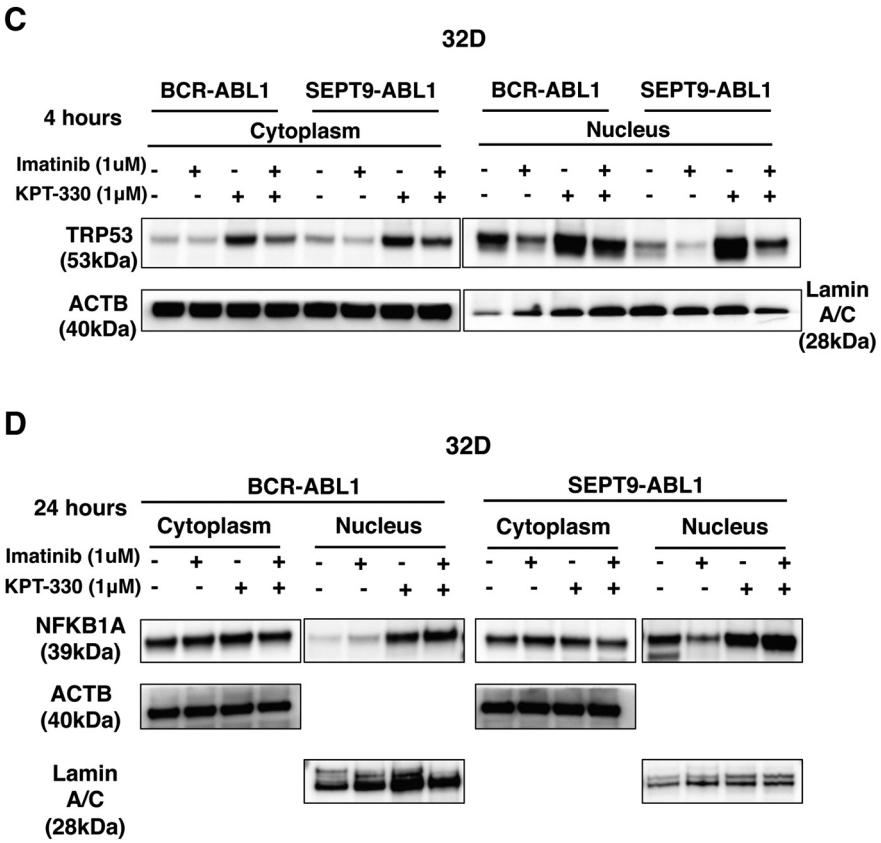

Figure 3. (*continued.*)

of the nuclear SET was greater after combination treatment than after treatment with KPT-330 alone (Figure 3*F*).

To evaluate the cellular response to KPT-330 in the combination with or without imatinib, 32D/BCR-ABL1 and 32D/SEPT9-ABL1 were cultured without treatment or with imatinib 1 μM, KPT-330 1 μM, or imatinib 1 μM plus KPT-330 1 μM. In 32D/BCR-ABL1 cells, imatinib or KPT-330 alone induced apoptosis, and the frequency of apoptotic cells was higher in the combination treatment than treated with either alone. In 32D/SEPT9-ABL1 cells, KPT-330 but not imatinib induced apoptosis. The frequency of apoptotic cells was higher in the combination treatment than treated with KPT-330 alone (Figure 3*H*). Similar results were demonstrated using BaF3/BCR-ABL1 and BaF3/SEPT9-ABL1 (Figure 3*I*).

These results demonstrated that CRM1 inhibitor KPT-330 inhibited the nuclear export of TRP53 directly or through the nuclear accumulation of NFKB1A and induced apoptosis in cells harboring SEPT9-ABL1 *in vitro*. Because the combination treatment was the most effective way to induce apoptosis, the nuclear accumulation of PP2A and SET was supposed to be important for inducing apoptosis in cells expressing SEPT9-ABL1.

The Effect of a CRM1 Inhibitor on Cells Harboring SEPT9-ABL1 In Vivo

Finally, we investigated the *in vivo* effects of a CRM1 inhibitor and its combination with imatinib using BaF3/SEPT9-ABL1 and 32D/SEPT9-ABL1 cells.

In the subcutaneous tumor model, imatinib treatment did not alter the tumor volume, and the tumor volume at day 22 was 132 mm^2. In contrast, the tumor volume after KPT-330 treatment was 75.6 mm^2 at day 22, which was significantly smaller than that after imatinib treatment (P = .030). The combination treatment further decreased the tumor volume to 38.5 mm^2 at day 22, which was also significantly smaller than that after imatinib treatment (P = .008), although no significant difference was noted between the volume after combination treatment and that after KPT-330 alone (Figure 4*A*).

In the intraperitoneal tumor model, we first confirmed that the intraperitoneallytransplanted BaF3/SEPT9-ABL1 cells systemically infiltrated afterward, making their way to bone marrow, spleen, and liver in the sacrificed moribund mice with hepatosplenomegaly (Figure 4*B*). When mice were treated with imatinib or KPT-330 alone, the median survival durations were 16 and 17 days, respectively, without any significant difference (P = .099). The median survival duration after the combination treatment of KPT-330 and imatinib was 20.5 days, which was significantly longer than that after treatment with imatinib (P = .004) or KPT-330 alone (P = .039) (Figure 4*C*). In 32D/SEPT9-ABL1 cells, the median survival duration with imatinib and KPT-330 alone was 23 and 28 days, respectively, and treatment with KPT-330 alone resulted in a significantly longer survival period than that with imatinib alone (P = .045). The median survival duration with the combination treatment with KPT-330 and imatinib was 29 days, which was significantly longer than that after treatment with imatinib (P = .005) or KPT-330 alone (P = .027) (Figure 4*D*).

These results indicated that combination treatment with KPT-330 and imatinib was more effective in reducing the leukemic cells harboring SEPT9-ABL1 *in vivo*, resulting in a prolonged survival in comparison to the imatinib alone.

Discussion

The current study found that the nuclear TP53 was downregulated and less phosphorylated in the cells expressing SEPT9-ABL1 than in

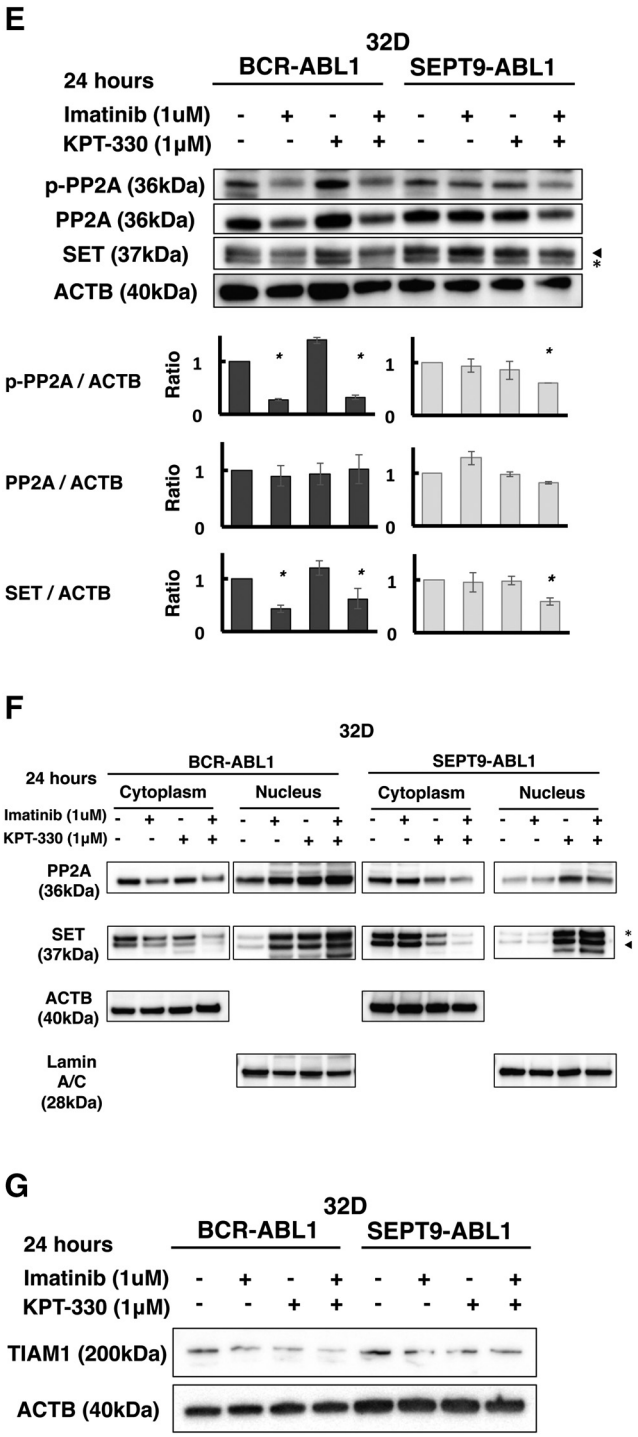

Figure 3. (*continued.*)

cells expressing BCR-ABL1, resulting in the prevention of apoptosis induced by TKIs. The administration of a CRM1 inhibitor, which suppresses the nuclear export of TP53 directly, or through the nuclear accumulation of NFKB1A, and causes the reactivation of PP2A, and the inhibition of SET expression successfully induced the apoptosis in the cells expressing SEPT9-ABL1 and inhibited their proliferation *in vivo*. Furthermore, combination therapy of a CRM1 inhibitor and imatinib was more effective in overcoming TKI resistance in cells expressing SEPT9-ABL1 than a CRM1 inhibitor.

Among the 10 *ABL1*-fusions reported thus far, only *SNX2-ABL1* and *SEPT9-ABL1* have exhibited resistance to TKIs natively. Both fusions had no point mutations in the catalytic domain of ABL1 [8,31], although such mutations have been reported in *BCR-ABL1* fusion from acquired TKI-resistant cells [32]. In *SNX2-ABL1*, both the SH2 and SH3 domains in ABL1, which are negative regulatory elements for the kinase domain, have been lost. The deficit of these SH2 and SH3 domains may promote the strong activation of ABL1 kinases, which may contribute to TKI resistance [33]. SEPT9-ABL1

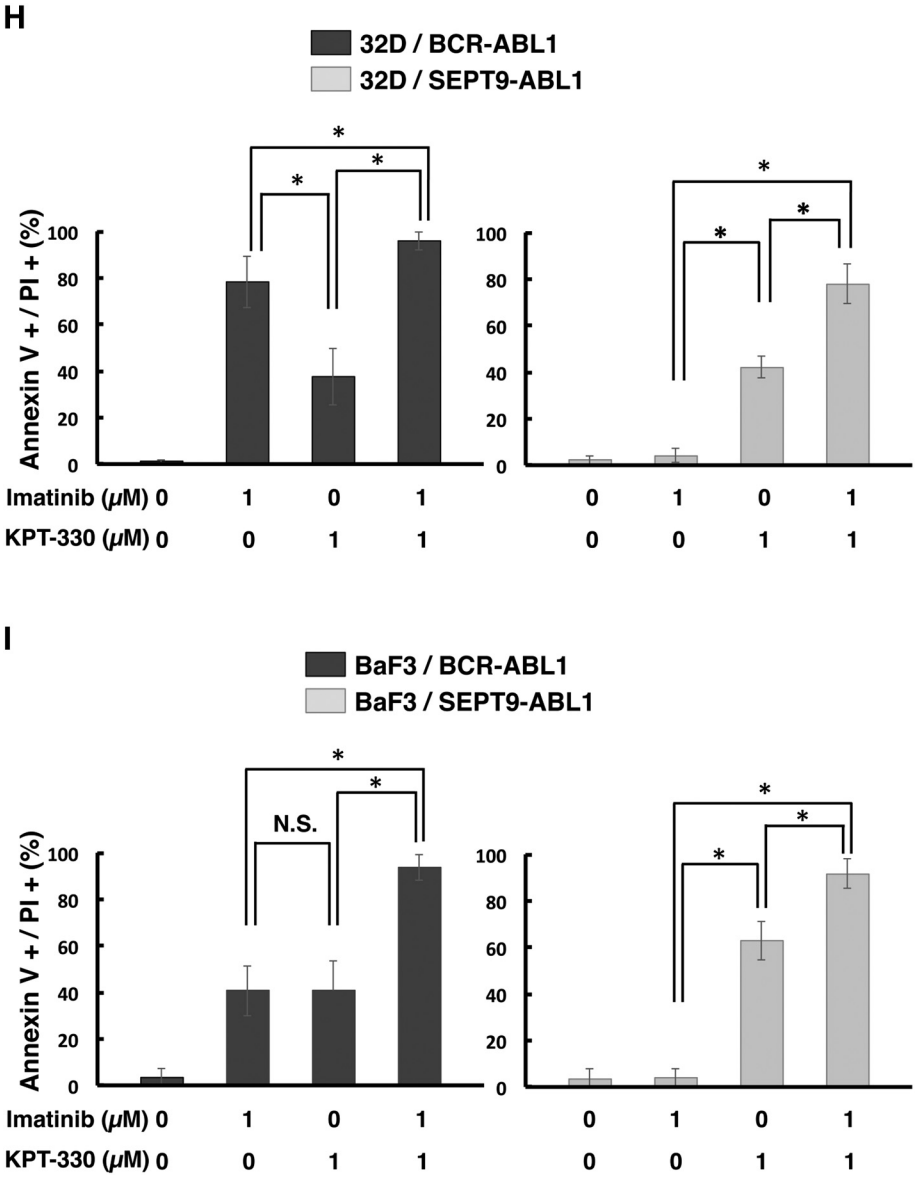

Figure 3. (*continued.*)

shares the ABL1 region harboring SH2 and SH3 domains with BCR-ABL1 with no point mutations. Although it is possible that the higher-order structure of SEPT9-ABL1 may be related to TKIs resistance, the mechanisms underlying TKI resistance from a molecular structure perspective have yet to be clarified.

BCR-ABL1 recruits and constitutively activates multiple signal pathways including the RAF/MEK/ERK pathway, JAK/STAT pathway, and PI3K/AKT pathway for consistent proliferation [34]. These signaling molecules have been examined as a target for treatment as well as overcoming TKI resistance [35–40]. The pro-survival protein kinase CK2 is a fascinating molecule that phosphorylates several targets, including RPS6, a common downstream effector of the RAF/MEK/ERK and PI3K/AKT pathways [41]. CK2 is highly expressed in CML progenitors [42] and even more highly expressed in the imatinib-resistant cells with *BCR-ABL1* gene amplification compared with imatinib-sensitive cells [43]. It interacts with BCR-ABL1, and the inhibition of CK2 restores TKIs sensitivity in cells with CK2 upregulation as well as without a high CK2 level [44]. The finding that a CK2 inhibitor was not effective in repressing the proliferation of cells harboring SEPT9-ABL1 suggests that while the RAF/MEK/ERK and PI3K/AKT pathways might not be involved in SEPT9-ABL1–induced TKIs resistance, other pathways might be involved, as was suggested by the strong phosphorylation of STAT5 in cells harboring SEPT9-ABL1 in our previous study [10].

The inhibition of BCR-ABL1 with TKIs has been reported to lead to the inactivation of MDM2 and activation of TP53 [45]. Furthermore, mutations or allelic losses of TP53 have been reported to be linked to the TKI resistance, progression to blast crisis, and a poor outcome in CML [12]. These findings suggest that the enhancement of the TP53 function may be a novel target in the treatment of TKI-resistant CML. MDM2 inhibitors have been proposed as a promising strategy for treating B-ALL, regardless of BCR-ABL1 [46]. However, the MDM2 inhibitors Nutlin-3a failed to overcome TKI resistance in cells harboring SEPT9-ABL1 in this study.

Another strategy for targeting TP53 is the application of CRM1 inhibitors. CRM1 is overexpressed in several hematologic and nonhematologic malignancies, and the upregulation of CRM1 is

correlated with a poor prognosis and drug resistance [47]. The SINE compounds KPT-251, KPT-276, and KPT-330, which interact with the NES-binding groove of CRM1 for nuclear export, are effective on acute leukemia, chronic lymphocytic leukemia, and multiple myeloma by inducing apoptosis [22,27,48,49]. The present data showed that KPT-330 effectively inhibited the cellular growth of cells

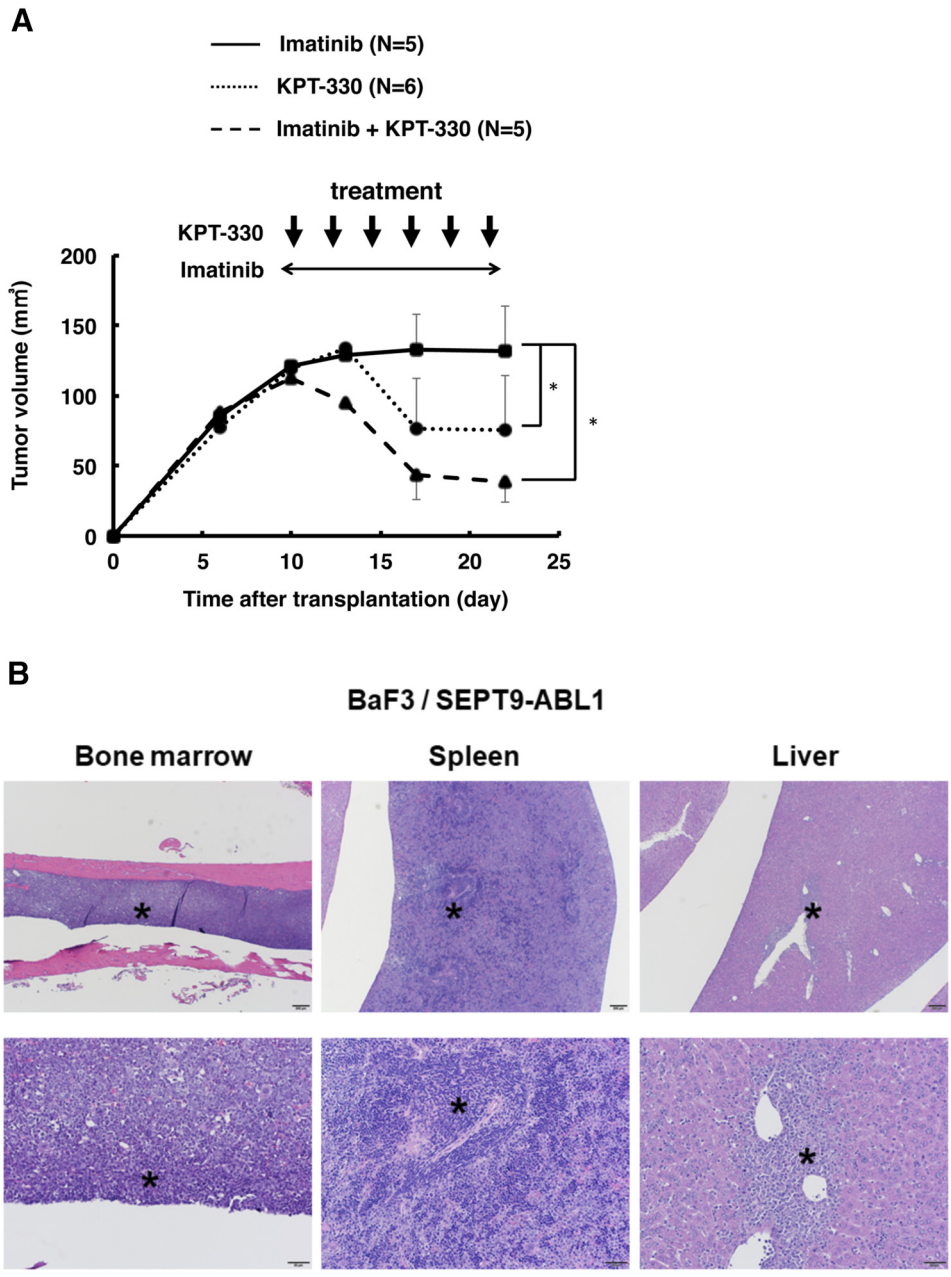

Figure 4. The effect of the CRM1 inhibitor on SEPT9-ABL1 *in vivo*.The changes in the tumor volume in the subcutaneous tumor model. BALB/c mice transplanted with 5×10^6 BaF3/SEPT9-ABL1 cells subcutaneously were treated with imatinib 20 mg/kg daily ($n = 5$), KPT-330 5mg/kg 3 times/week (n 6), or imatinib 20mg/kg daily and KPT-330 5mg/kg 3 times/week ($n = 5$) from 10 days after transplantation. The calculated volume of the subcutaneous tumors is indicated at the vertical axis. * indicates a P value <.05.(B) The pathohistology of the involved organs in leukemic mice with BaF3/SEPT9-ABL1 cells. The histological sections stained with hematoxylin and eosin are shown. BaF3/SEPT9-ABL1 cells infiltrated diffusely throughout the bone marrow, predominantly in the red pulp of spleen, and the lobules as well as around the vessels and Glisson's sheath in the liver. * indicates tumor cells. The magnification ratio was showed at 20× in the upper figures and at 100× in the lower figure. The bars indicate 200 μm in the upper figures and 50 μm in the lower figures.(C) The Kaplan-Meier survival curves of the intraperitoneal tumor model. BALB/c mice transplanted with 2×10^6 BaF3/SEPT9-ABL1 cells intraperitoneally were treated with vehicle ($n = 3$), imatinib 20 mg/kg daily ($n = 7$), KPT-330 50 mg/kg 3 times/week ($n = 8$), or imatinib 20 mg/kg daily and KPT-330 50 mg/kg 3 times/week ($n = 12$) from the day after transplantation. * indicates a P value <.05 (imatinib and KPT-330 *vs.* imatinib), and **indicates a P value <.05 (imatinib and KPT-330 *vs.* KPT-330).(D) The Kaplan-Meier survival curves of the intraperitoneal tumor model. BALB/c mice transplanted with 2 10^6 32D/SEPT9-ABL1 cells intraperitoneally were treated with vehicle ($n = 3$), imatinib 20 mg/kg daily ($n = 7$), KPT-330 50 mg/kg 3 times/week ($n = 7$), or imatinib 20 mg/kg daily and KPT-330 50 mg/kg 3 times/week ($n = 8$) from the day after transplantation. * indicates a P value <.05 (imatinib and KPT-330 *vs.* imatinib), **indicates a P value <.05 (imatinib and KPT-330 *vs.* KPT-330), and ***indicates a P value <.05 (imatinib *vs.* KPT-330).

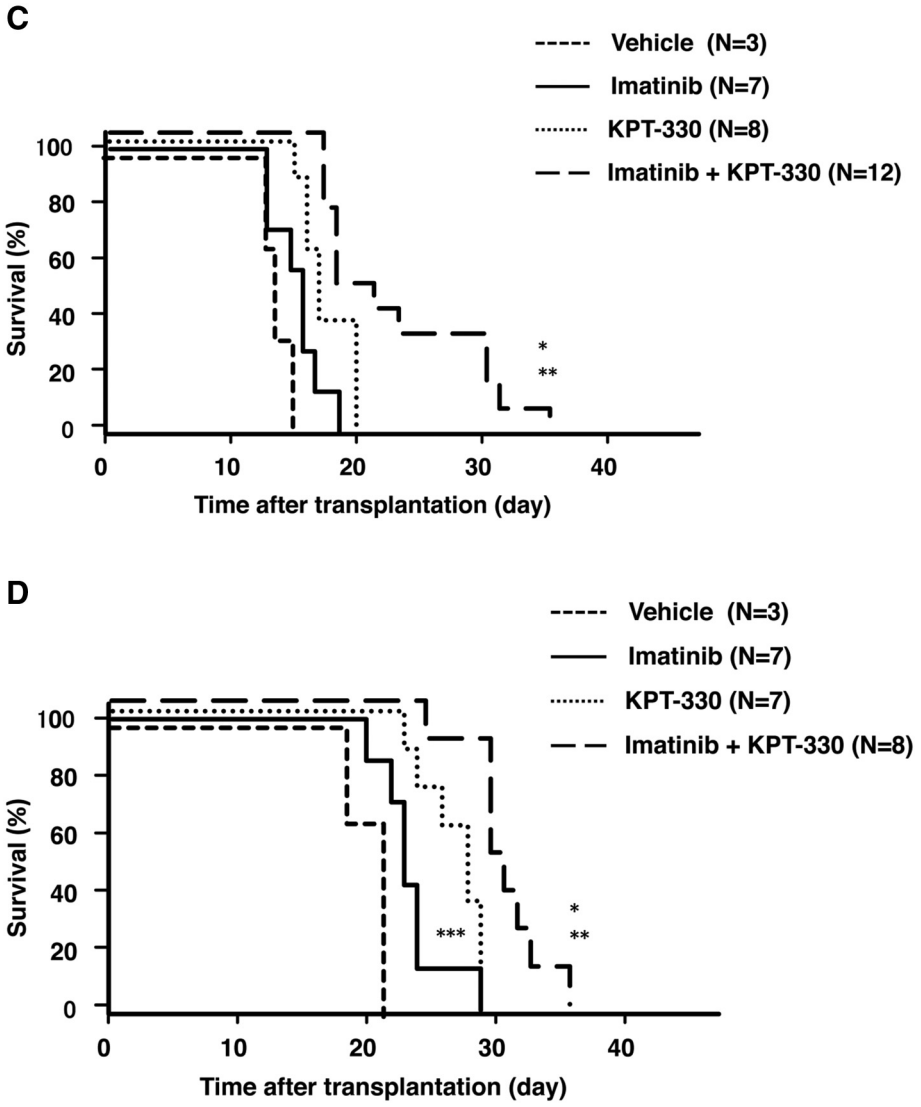

Figure 4. (*continued.*)

harboring SEPT9-ABL1 *in vitro* and *in vivo*. Because KPT-330 but not the MDM2-specific inhibitor Nutlin-3a was effective, KPT-330 might inhibit the key molecular changes induced by CRM1 that mediate the SEPT9-ABL1 function cooperatively, including the export of TP53 as well as the alteration of other molecules, such as NFKB1A, PP2A, and SET, as shown in this study. These molecules also have an important role in nonhematologic malignancies: the loss NFKB1A causes resistance to TKIs in EGFR mutant lung cancer [50], and CRM1 inhibition is effective through inducing intolerance of nuclear NFKB1A accumulation in KRAS mutant lung cancer [51]. PP2A and SET are involved in EGFR or KRAS-driven lung tumorigenesis [52]. TIAM1, which is inhibited by PP2A, is required for EGFR-induced tumorigenesis [30]. Although it remains unclear to what extent each kind of molecule contributes to tumorigenesis with SEPT9-ABL1, it is suggested that the nuclear accumulation and the resulting functional alteration of these molecules including TP53 induced by CRM1 inhibition comprehensively achieve a regression of the leukemic cells harboring SEPT9-ABL1.

In conclusion, the SEPT9-ABL1, which possesses the same ABL1 structure as BCR-ABL1 but a different N-terminal, induced the low expression of TP53 and TKI resistance. A CRM1 inhibitor administered in combination with imatinib was an effective method of overcoming the TKI resistance of SEPT9-ABL1. CRM1 inhibitors are fascinating and a potentially useful strategy that affects several key molecules, including the nuclear accumulation of TP53. Further analyses and refinement of CRM1 inhibitors will facilitate their application in the treatment of various malignancies in the future.

Author Contributions

H.K.: collection and assembly of data, data analysis and interpretation, and manuscript writing; H.M.: conception and design, collection and assembly of data, data analysis and interpretation, and manuscript writing; R.S., Y.K., Y.O., and H.K.: collection and assembly of the data; K.A.: conception and design, administrative support, data analysis and interpretation, manuscript writing, and final approval of manuscript.

Acknowledgements

We thank Dr. Toshio Kitamura (The University of Tokyo) for providing the PLAT-gp packaging cells; Dr. Masatoshi Ito for his professional technical assistance and valuable advice; and Ms. Akemi Kamijo, Ms. Katsuko Naito, and Ms. Yoshiko Ito (Support Center

for Medical Research and Education, Tokai University) for their professional technical assistance. This work was supported by a Grant-in-Aid for Scientific Research from the Ministry of Education, Culture, Sports, Science, and Technology of Japan (K.A.); Tokai University School of Medicine Project Research (H.K.); and Research and Study Program of Tokai University Educational System General Research Organization (H.K.).

Disclosure of Potential Conflicts of Interest

The authors declare no potential conflicts of interest.

References

[1] De Braekeleer E, Douet-Guilbert N, Rowe D, Bown N, Morel F, Berthou C, Férec C, and De Braekeleer M (2011). ABL1 fusion genes in hematological malignancies: a review. *Eur J Haematol* **86**, 361–371.

[2] Melo JV and Deininger MW (2004). Biology of chronic myelogenous leukemia—signaling pathways of initiation and transformation. *Hematol Oncol Clin North Am* **18**, 545–568.

[3] Hochhaus A, Baccarani M, Deininger M, Apperley JF, Lipton JH, Goldberg SL, Corm S, Shah NP, Cervantes F, and Silver RT, et al (2008). Dasatinib induces durable cytogenetic responses in patients with chronic myelogenous leukemia in chronic phase with resistance or intolerance to imatinib. *Leukemia* **22**, 1200–1206.

[4] Saglio G, Kim DW, Issaragrisil S, le Coutre P, Etienne G, Lobo C, Pasquini R, Clark RE, Hochhaus A, and Hughes TP, et al (2010). Nilotinib versus imatinib for newly diagnosed chronic myeloid leukemia. *N Engl J Med* **362**, 2251–2259.

[5] Chiaretti S and Foa R (2015). Management of adult Ph-positive acute lymphoblastic leukemia. *Hematology Am. So.c Hematol. Educ. Dent Prog* **2015**, 406–413.

[6] Greuber EK, Smith-Pearson P, Wang J, and Pendergast AM (2013). Role of ABL family kinases in cancer: from leukaemia to solid tumours. *Nat Rev Cancer* **13**, 559–571.

[7] Deenik W and Beverloo HB (2009). van der Poel-van de Luytgaarde SC, Wattel MM, van Esser JW, Valk PJ, Cornelissen JJ. Rapid complete cytogenetic remission after upfront dasatinib monotherapy in a patient with a NUP214-ABL1-positive T-cell acute lymphoblastic leukemia. *Leukemia* **23**(3), 627–629.

[8] Suzuki R, Matsushita H, Kawai H, Matsuzawa H, Tsuboi K, Watanabe S, Kawada H, Ogawa Y, and Ando K (2014). Identification of a novel SEPT9-ABL1 fusion gene in a patient with T-prolymphocytic leukemia. *Leuk Res Rep* **3**, 54–57.

[9] Hall PA and Russell SE (2004). The pathobiology of the septin gene family. *J Pathol* **204**, 489–505.

[10] Kawai H, Matsushita H, Suzuki R, Sheng Y, Lu J, Matsuzawa H, Yahata T, Tsuma-Kaneko M, Tsukamoto H, and Kawada H, et al (2014). Functional analysis of the SEPT9-ABL1 chimeric fusion gene derived from T-prolymphocytic leukemia. *Leuk Res* **38**, 1451–1459.

[11] Quintás-Cardama A and Cortes J (2009). Molecular biology of bcr-abl1–positive chronic myeloid leukemia. *Blood* **113**, 1619–1630.

[12] Wendel HG, de Stanchina E, Cepero E, Ray S, Emig M, Fridman JS, Veach DR, Bornmann WG, Clarkson B, and McCombie WR, et al (2006). Loss of p53 impedes the antileukemic response to BCR-ABL inhibition. *Proc Natl Acad Sci U S A* **103**, 7444–7449.

[13] Cox ML and Meek DW (2010). Phosphorylation of serine 392 in p53 is a common and integral event during p53 induction by diverse stimuli. *Cell Signal* **22**, 564–571.

[14] Moll UM and Petrenko O (2003). The MDM2-p53 interaction. *Mol Cancer Res* **1**, 1001–1008.

[15] Schmitt CA, Fridman JS, Yang M, Baranov E, Hoffman RM, and Lowe SW (2002). Dissecting p53 tumor suppressor functions in vivo. *Cancer Cell* **1**, 289–298.

[16] Buontempo F, McCubrey JA, Orsini E, Ruzzene M, Cappellini A, Lonetti A, Evangelisti C, Chiarini F, Evangelisti C, and Barata JT, et al (2018). Therapeutic targeting of CK2 in acute and chronic leukemias. *Leukemia* **32**, 1–10.

[17] Shangary S and Wang S (2009). Small-molecule inhibitors of the MDM2-p53 protein-protein interaction to reactivate p53 function: a novel approach for cancer therapy. *Ann Rev Pharmacol Toxicol* **49**, 223–241.

18 Ishizawa J, Kojima K, Hail Jr N, Tabe Y, and Andreeff M (2015). Expression, function, and targeting of nuclear exporter chromosome region maintenance 1 (CRM1) protein. *Pharmacol Ther* **153**, 25–35.

[19] Fukuda M, Asano S, Nakamura T, Adachi M, Yoshida M, Yanagida M, and Nishida E (1997). CRM1 is responsible for intracellular transport mediated by the nuclear export signal. *Nature* **390**, 308–311.

[20] Etchin J, Sun Q, Kentsis A, Farmer A, Zhang ZC, Sanda T, Mansour MR, Barcelo C, McCauley D, and Kauffman M (2013). Antileukemic activity of nuclear export inhibitors that spare normal hematopoietic cells. *Leukemia* **27**, 66–74.

[21] Lapalombella R, Sun Q, Williams K, Tangeman L, Jha S, Zhong Y, Goettl V, Mahoney E, Berglund C, and Gupta S (2012). Selective inhibitors of nuclear export show that CRM1/XPO1 is a target in chronic lymphocyticleukemia. *Blood* **120**, 4621–4634.

[22] Ranganathan P, Yu X, Na C, Santhanam R, Shacham S, Kauffman M, Walker A, Klisovic R, Blum W, and Caligiuri M (2012). Preclinicalactivity of a novel CRM1 inhibitor in acute myeloid leukemia. *Blood* **120**, 1765–1773.

[23] Crivellaro S, Panuzzo C, Carrà G, Volpengo A, Crasto F, Gottardi E, Familiari U, Papotti M, Torti D, and Piazza R, et al (2015). Non genomic loss of function of tumor suppressors in CML: BCR-ABL promotes IκBα mediated p53 nuclear exclusion. *Oncotarget* **6**(28), 25217–25225.

[24] Ming M, Wu W, Xie B, Sukhanova M, Wang W, Kadri S, Sharma S, Lee J, Shacham S, and Landesman Y, et al (2018). XPO1 inhibitor selinexor overcomes intrinsic ibrutinib resistance in mantle cell lymphoma via nuclear retention of IκB. *Mol Cancer Ther* **17**(12), 2564–2574.

[25] Kuruvilla J, Savona M, Baz R, Mau-Sorensen PM, Gabrail N, Garzon R, Stone R, Wang M, Savoie L, and Martin P, et al (2017). Selective inhibition of nuclear export with selinexor in patients with non-Hodgkin lymphoma. *Blood* **129**(24), 3175–3183.

[26] Body S, Esteve-Arenys A, Miloudi H, Recasens-Zorzo C, Tchakarska G, Moros A, Bustany S, Vidal-Crespo A, Rodriguez V, and Lavigne R, et al (2017). Cytoplasmic cyclin D1 controls the migration and invasiveness of mantle lymphoma cells. *Sci Rep* **7**(1)13946.

[27] Walker CJ, Oaks JJ, Santhanam R, Neviani P, Harb JG, Ferenchak G, Ellis JJ, Landesman Y, Eisfeld AK, and Gabrail NY (2013). Preclinical and clinical efficacy of XPO1/CRM1 inhibition by the karyopherin inhibitor KPT-330 in Ph + leukemias. *Blood* **122**, 3034–3044.

[28] Neviani P, Santhanam R, Trotta R, Notari M, Blaser BW, Liu S, Mao H, Chang JS, Galietta A, and Uttam A (2005). The tumor suppressor PP2A is functionally inactivated in blast crisis CML through the inhibitory activity of the BCR/ABL-regulated SET protein. *Cancer Cell* **8**, 355–368.

[29] Hofbauer SW, Krenn PW, Ganghammer S, Asslaber D, Pichler U, Oberascher K, Henschler R, Wallner M, Kerschbaum H, and Greil R, et al (2014). Tiam1/Rac1 signals contribute to the proliferation and chemoresistance, but not motility, of chronic lymphocytic leukemia cells. *Blood* **123**(14), 2181–2188.

[30] Zhu G, Fan Z, Ding M, Zhang H, Mu L, Ding Y, Zhang Y, Jia B, Chen L, and Chang Z, et al (2015). An EGFR/PI3K/AKT axis promotes accumulation of the Rac1-GEF Tiam1 that is critical in EGFR-driven tumorigenesis. *Oncogene* **34** (49), 5971–5982.

[31] Masuzawa A, Kiyotani C, Osumi T, Shioda Y, Iijima K, Tomita O, Nakabayashi K, Oboki K, Yasuda K, and Sakamoto H (2014). Poor responses to tyrosine kinase inhibitors in a child with precursor B-cell acute lymphoblastic leukemia with SNX2-ABL1 chimeric transcript. *Eur J Haematol* **92**, 263–267.

[32] Soverini S, Hochhaus A, Nicolini FE, Gruber F, Lange T, Saglio G, Pane F, Müller MC, Ernst T, and Rosti G (2011). BCR-ABL kinase domain mutation analysis in chronic myeloid leukemia patients treated with tyrosine kinase inhibitors: recommendations from an expert panel on behalf of European LeukemiaNet. *Blood* **118**, 1208–1215.

[33] Tomita O, Iijima K, Ishibashi T, Osumi T, Kobayashi K, Okita H, Saito M, Mori T, Shimizu T, and Kiyokawa N (2014). Sensitivity of SNX2-ABL1 toward tyrosine kinase inhibitors distinct from that of BCR-ABL1. *Leuk Res* **38**, 361–370.

[34] Cilloni D and Saglio G (2012). Molecular pathways: BCR-ABL. *Clin Cancer Res* **18**, 930–937.

[35] Eiring AM, Page BDG, Kraft IL, Mason CC, Vellore NA, Resetca D, Zabriskie MS, Zhang TY, Khorashad JS, and Engar AJ (2015). Combined STAT3 and BCR-ABL1 inhibition induces synthetic lethality in therapy-resistant chronic myeloid leukemia. *Leukemia* **29**(587–597).

[36] Gleixner KV, Schneeweiss M, Eisenwort G, Berger D, Herrmann H, Blatt K, Greiner G, Byrgazov K, Hoermann G, and Konopleva M (2017). Combined targeting of STAT3 and STAT5: a novel approach to overcome drug resistance in chronic myeloid leukemia. *Haematologica* **102**(948–957).

[37] Chorzalska A, Ahsan N, Rao RSP, Roder K, Yu X, Morgan J, Tepper A, Hines S, Zhang P, and Treaba DO (2018). Overexpression of Tpl2 is linked to imatinib resistance and activation of MEK-ERK and NF-κB pathways in a model of chronic myeloid leukemia. *Mol Oncol* **12**, 630–647.

[38] Airiau K, Turcq B, Mahon FX, and Belloc F (2017). A new mechanism of resistance to ABL1 tyrosine kinase inhibitors in a BCR-ABL1–positive cell line. *Leuk Res* **61**, 44–52.

[39] Wagle M, Eiring AM, Wongchenko M, Lu S, Guan Y, Wang Y, Lackner M, Amler L, Hampton G, and Deininger MW (2016). A role for FOXO1 in BCR-ABL1–independent tyrosine kinase inhibitor resistance in chronic myeloid leukemia. *Leukemia* **30**, 1493–1501.

[40] Leo E, Mancini M, Aluigi M, Luatti S, Castagnetti F, Testoni N, Soverini S, Santucci MA, and Martinelli G (2013). BCR-ABL1–associated reduction of beta catenin antagonist Chibby1 in chronic myeloid leukemia. *PLoS One* **8**e81425.

[41] Salizzato V, Borgo C, Cesaro L, Pinna LA, and Donella-Deana A (2016). Inhibition of protein kinase CK2 by CX-5011 counteracts imatinib-resistance preventing rpS6 phosphorylation in chronic myeloid leukaemia cells: new combined therapeutic strategies. *Oncotarget* **7**, 18204–18218.

[42] Morotti A, Carrà G, Panuzzo C, Crivellaro S, Taulli R, Guerrasio A, and Saglio G (2015). Protein kinase CK2: a targetable BCR-ABL partner in Philadelphia positive leukemias. *Adv Hematol* **612567**(2015).

[43] Borgo C, Cesaro L, Salizzato V, Ruzzene M, Massimino ML, Pinna LA, and Donella-Deana A (2013). Aberrant signalling by protein kinase CK2 in imatinib-resistant chronic myeloid leukaemia cells: biochemical evidence and therapeutic perspectives. *Mol Oncol* **7**, 1103–1115.

[44] Hériché JK and Chambaz EM (1998). Protein kinase CK2alpha is a target for the Abl and Bcr-Abl tyrosine kinases. *Oncogene* **17**, 13–18.

[45] Goetz AW, van der Kuip H, Maya R, Oren M, and Aulitzky WE (2001). Requirement for Mdm2 in the survival effects of Bcr-Abl and interleukin 3 in hematopoietic cells. *Cancer Res* **61**, 7635–7641.

[46] Trino S, De Luca L, Laurenzana I, Caivano A, Del Vecchio L, Martinelli G, and Musto P (2016). P53-MDM2 pathway: evidences for a new targeted therapeutic approach in B-acute lymphoblastic leukemia. *Front Pharmacol* **7**(491).

[47] Kojima K, Kornblau SM, Ruvolo V, Dilip A, Duvvuri S, Davis RE, Zhang M, Wang Z, Coombes KR, and Zhang N (2013). Prognostic impact and targeting of CRM1 in acute myeloid leukemia. *Blood* **121**, 4166–4174.

[48] Lapalombella R, Sun Q, Williams K, Tangeman L, Jha S, Zhong Y, Goettl V, Mahoney E, Berglund C, and Gupta S (2012). Selective inhibitors of nuclear export show that CRM1/XPO1 is a target in chronic lymphocytic leukemia. *Blood* **120**, 4621–4634.

[49] Tai YT, Landesman Y, Acharya C, Calle Y, Zhong MY, Cea M, Tannenbaum D, Cagnetta A, Reagan M, and Munshi AA (2014). CRM1 inhibition induces tumor cell cytotoxicity and impairs osteoclastogenesis in multiple myeloma: molecular mechanisms and therapeutic implications. *Leukemia* **28**, 155–165.

[50] Bivona TG, Hieronymus H, Parker J, Chang K, Taron M, Rosell R, Moonsamy P, Dahlman K, Miller VA, and Costa C, et al (2011). FAS and NF-κB signalling modulate dependence of lung cancers on mutant EGFR. *Nature* **471**(7339), 523–526.

[51] Kim J, McMillan E, Kim HS, Venkateswaran N, Makkar G, Rodriguez-Canales J, Villalobos P, Neggers JE, Mendiratta S, and Wei S, et al (2016). XPO1-dependent nuclear export is a druggable vulnerability in KRAS-mutant lung cancer. *Nature* **538**(7623), 114–117.

[52] Zhou X, Updegraff BL, Guo Y, Peyton M, Girard L, Larsen JE, Xie XJ, Zhou Y, Hwang TH, and Xie Y, et al (2017). PROTOCADHERIN 7 acts through SET and PP2A to potentiate MAPK signaling by EGFR and KRAS during lung tumorigenesis. *Cancer Res* **77**(1), 187–197.